Oscar Alvarez[1], Ana Delia Contreras[1] and Tomás Morales[2]

Statistical and Dynamical Interpretation of the Midsummer Drought in Eastern Mexico

[1] Licenciatura de Ciencias Atmosféricas, Universidad Veracruzana, Jalapa, MEXICO.
[2] Facultad de Biología, Universidad Autónoma de Tlaxcala, Campus Ixtlacuixtla.

Abstract Spectral analysis of time series in the eastern Mexico shows a new face of the behavior of rainfall in the wet season. The impact in the three states sector knows as PTV (Puebla-Tlaxcala-Veracruz) is evaluated. The NCAR/ NCEP reanalysis model and other documented datasets are applied. The instantaneous phase of Hilbert transform derived from rainfall time series allows simplifying the analysis of variability, making correspond to synoptic fluctuations Hovmoller diagrams show that temporal scale varying from weekly to daily or even hourly. Wet and dry spells progression reveals strong seasonality, lack of gaussianity, space-time disaggregation and non-stationary. The impact of midsummer drought over crop yields result highly correlated with kinematics features of zonal wind at 850 HPa. Finally, the higher resolution in spatial and temporal scales leads to a new perspective of the midsummer drought in eastern Mexico.

1. Introduction

The rainy season of eastern Mexico begins in May and ends in October. Rainfall thought wet season is dominated by several transient perturbations. The most important of these perturbations are the meridional shift of the intertropical convergence zone (ITCZ), located at the southern of Mexican country. The subtropical high pressure systems (SHPS) from North Atlantic and eastern Pacific are also contributed to the climate in summer (Gianni *et al*., 2000).

The region under study (Fig. 1.1) is located in the eastern of the country. The area is about 487,454 km^2 and is formed by a tree states: Puebla, Tlaxcala y Veracruz (PTV). Puebla is a state located in the central Altiplano. The climate in this region is influenced for eastern Pacific and Gulf of Mexico. Temperatures vary widely 6 to 27^o C and have a wet season of about 200 mm and 1193 mm per year. Tlaxcala is a tiny state in the Altiplano of Central Mexico and situated in the Transversal Neo-volcanic Axis, where elevations range from 2000 to over 4000 meters above sea level.

Temperatures vary 5 to 25^{o}C .The wet season is about 120 mm and 693 mm per year. Drought is also common, particularly in the north and eastern parts of Tlaxcala. The importance of include Tlaxcala is because form an edge into a large region affected by the mid-summer drought. The third state included in PTV is Veracruz, a coastal region at southwest margin of Gulf of Mexico. Temperatures vary 11 to 26^{o}C and have a wet season of about 234 mm and 1460 mm per year. The atmospheric circulation in PTV zone is controlled by the competition between the SHPS at sea level and the eastern Pacific ITCZ. Additional influences are derived from tropical waves (Salinas, 2006). The rainfall climatology of Mexico display remarkable spatial variations (Pavia *et al*., 2006; Larson *et al*., 2005).

Variations in both seasonal amounts and the timing of rainfall within the season certainly influence the production of maize. Several recent studies trace teleconnections with ENSO. This teleconnections are over regional and subregional scale. The effect of ENSO can further be complicated by the presence of topography, as in Costa Rica (Waylen *et al*. 1996). The intensification of the trade winds, from the Caribbean basin westward toward the eastern Pacific ITCZ, acts in conjunction with topographic uplift to increase rainfall totals on the Caribbean coast, while simultaneously decreasing them on the Pacific one.

The annual cycle of precipitation over the southern Mexico and Central America exhibits a bimodal distribution with maxima during June and September–October and a relative minimum during July and August, known as the midsummer drought (MSD). Is well known that the secondary rainfall minimum in July–August, is explained in terms of a westward enhancement of the subtropical high.

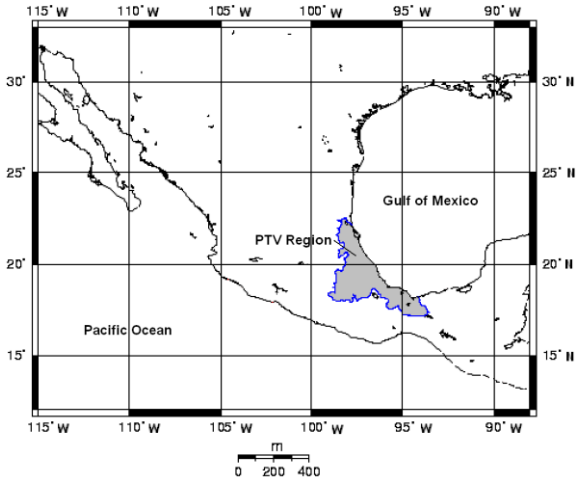

Fig. 1.1 The region of interest in the Eastern Mexico

The MSD signal can also be detected trough other variables: minimum and maximum surface temperature and even in tropical cyclone activity over the eastern Pacific. Analyses on the dynamics of the MSD are relatively scarce. Magaña *et al*. (1999) propose a mechanism to explain the dynamics of this phenomenon with atmosphere–ocean–land processes. The spatial resolution employed in Magaña's paper is broad in scale ($5^{o}\times5^{o}$) and bulky in time domain (biweekly).

In recent years impressive evidence has accumulated to support new ideas that the MSD signatures are controlled for periodic perturbations in the trade winds. Previous studies have revealed key aspects of the summertime rainfall on the eastern Mexico. Over the past two decades, numerous studies have demonstrated that Madden–Julian oscillation (MJO) is the dominant mode of the intraseasonal (30–60 days) atmospheric variability within the tropical troposphere. The MJO form a planetary-scale disturbance in both tropical deep convection and tropospheric circulation, which propagates eastward along the equator in a complete cycle around the globe lasting approximately 30–60 days (Madden and Julian, 1994). The observational measures of the MJO activity showed large interanual variations. MJO, as depicted from distinct empirical and modeling methods, evidenced largest amplitudes of the intraseasonal anomalies extending across the warm pool region between the Indian and western Pacific Oceans (Kayano and Kousky, 1999; Matthews, 2000).

This paper explores other views in intraseasonal variability in eastern Mexico's warm season rainfall. To evaluate the temporal variability in the rainfall, a new set of statistical tools are employed. We adopt a high resolution perspective to the intrinsic complexities of summer rainfall over central and eastern Mexico. The focus here is on basin-scale conditions, since large-scale circulation patterns associated with wet and dry conditions on the central Mexico are described elsewhere.

It applies a time dependent techniques for displaying climatic data and a more sophisticated numerical algorithms on rainfall time series. This study investigates the MSD with daily and hourly rainfall data from reanalysis (Kalnay *et al*., 1996), in situ conventional data banks and other external sources. The innovations explored here are Hovmoller diagrams, wavelets analysis and Hilbert transforms. These different analytical techniques tend to quantify and simplify the description of meteorological events.

Advancing technology provides ever more abundant and effective ways to gather measurement data. Skillfulness is required for processing and interpretation. Two independent disciplines have recently emerged that fit these tasks: visualization (Nielsen-Gammon, 2001) and multiresolution signal analysis (Coulibaly and Burn, 2005). Scientific visualization draws on elements of many established techniques to provide methods for presenting complex and voluminous data. Visualization uses the supremacy of human visual cognition to expand the raw computation abilities of computers. On the other side, multiresolution signal combines methods originating from applied mathematics to create a new set of tools capable to attain a multilevel detail.

In the statistical point of view two tools are revisited: wavelets and Hilbert transforms. The wavelet analysis is the basic tool to define the regional structure of summer rainfall. The wavelet transform is an analytical instrument that divides data (functions or operators) into different frequency components, and then permits the study of each component with a resolution matched to its scale (Anctil and Coulibaly, 2004). It has advantage over typical spectral analysis, because it allows analyzing different scales of temporal variability and it does not need a stationary series. Thus, it is suitable to scrutinize unregular distributed events and time series that contain nonstationary power over a wide range of frequencies. Then, it is becoming a common tool for analyzing localized variations of power within a time series. In rainfall studies (Santos *et al*., 2001) the wavelet transform has shown variability parameters. Other applications are tropical convection (Mwale and Gan, 2005), ENSO signal detection (Lau and Weng, 1995), atmospheric cold fronts and temperature variability (Torrence y Compo, 1998).

The present work is organized as follows. In Sect. 2 we present all data sources employed. In the section 3 are plotted and synthesized the results obtained with Hövmoller diagrams. The wavelet analysis is presented in section 4. The Hilbert transform methods and results are shown in section 5. The section 6 condenses the discussion in dynamical variables and reanalysis. In section 7 are presented the discussion, and finally the conclusions of the work are drawn in section 8.

2. Data

The source of data are multiple : [1] North American Regional Reanalysis (Mesinger et al., 2006) from the Web page http://www.emc.ncep.noaa.gov/mmb/rreanl/, [2] GES-DISC Interactive Online Visualization ANd aNalysis Infrastructure (Giovanni) as part of the NASA's Goddard Earth Sciences (GES) Data and Information Services Center (DISC) [3] Fast Extractor of Climate Information ERIC II, [4] Climate Information from manual stations of the Mexican Weather Service from the Sate of Tlaxcala (ECET).

3. Hövmoller diagrams

Hövmoller diagrams (HODS) are common tools in climate research (Martius et al., 2006), and is particularly useful for summarizing quasi-two-dimensional regimes and detect variations over time and space. HODS can abridge massive amounts of data in crisp fashion, since relevant information is lost in averaging process. These data presentations have become so ubiquitous in data analysis. HODS can be constructed using time-longitude or time-latitude for rainfall plots. High efficiency was proved in a warm season precipitation scenario because indicate short and long-lived coherent episodes. This technique is plenty precise for both statistical and dynamical interpretation of MSD and relatively modest work has been done on periodicities from a week or two to several months. The reasons are complex. In part, it is because the combinations of synoptic fluctuations in the weather and the annual march of the seasons make this shorter-term cycles more difficult to detect (Jury and Pathak, 1991).

4. Wavelet analysis

Mathematical transformations are applied to signals to obtain further information from that signal that is not readily available in the raw signal. The use of wavelets as a tool for time series analysis and signal processing has increased in recent years due to their potential for solving a number of practical problems (Ghil et al., 2002). In particular, wavelets can decompose the variance of a physical process across different scales and have been used in this way in a number of scientific and engineering disciplines. The wavelet analysis (WAN) is applied in monsoon variability problems (Nolin and Hall-McKim, 2006). An important parameter of a typical WAN is the variance. Roughly speaking, the variance is a measure of how much a weighted average with bandwidth λ changes form one time period of length λ to the next. The wavelet variance decomposes the variance of a time series into components associated with different scales. A region of linear variation on a plot of logarithm of variance, indicates the existence of a

power law behavior (Joseph et al., 2000), and the slope of the line can be used to deduce the exponent α.

Let V(TL) the variance of the global wavelet defined as follows:

$$V(T_L) = \int_{t_1}^{t_2} P(t, T_L)\, dt \qquad (\mathbf{4.1})$$

Herein T_L represents the period and t_1 y t_2 indicates the "initial" and "final" time in the time series. $P(t,T_L)$ is the function associated with the continuous wavelet spectrum.

5. Hilbert Transform

Climatic signals are statistical elements in studying variability, impacts (Greenland, 2005) climate change (Hegerl et al., 2004) and fine-scale regional signature of some prominent oscillations (Bojariu and Giorgi, 2005). The Hilbert transform (HT) methods are recently used in earth sciences (Mélice et al., 2001) and applied to non-periodical signal of nonlinear response systems. In meteorology HT analysis is capable to develop signatures of synoptic phenomena, ocean tides, and intricate patterns of precipitation (Duffy, 2004).

The HT theory is poorly known and belongs to no conventional background for many specialists in climate analysis. However, the basic scheme is simple. Suppose that a real function x(t) can be expressed in the form

$$x(t) = a(t)\cos\phi(t) \qquad (\mathbf{5.1})$$

where a(t) is called as instantaneous amplitude and ϕ(t) the instantaneous phase (Picinbono, 1997). The canonical pair [a(t), ϕ(t)] represent in an unambiguous way x(t), introducing the analytical signal z(t):

$$z(t) = x(t) + i\, H[x(t)], \qquad (\mathbf{5.2})$$

Where

$$i = \sqrt{-1}$$

$$H[x(t)] = \frac{1}{\pi} P \int_{-\infty}^{\infty} \frac{x(s)}{t-s}\, ds \qquad (\mathbf{5.3})$$

H is called the Hilbert Transform of x(t) and P the Cauchy's main value of the integral. Hilbert Transform converts any cosenoidal term into a senoidal term. Since Sin (ωt) = Cos (ωt – 0.5π) and – Cos (ωt) = Sin (ωt – 0.5π) the HT is associated with a phase change –0.5π (– 90º) of whole harmonics in the Fourier image. Im{z(t)} and Re{z(t)}form an orthogonal basis and z(t) is the phasor in the complex plane {x(t),H{x(t)}:

$$H[x(t)] = a(t)\sin\phi(t) \qquad (\mathbf{5.4})$$

$$z(t) = a(t)\, e^{\phi(t)}$$

Thus

$$a(t) = \sqrt{x^2(t) + H^2[x(t)]} \qquad (\mathbf{5.5})$$

and

$$\phi(t) = \tan^{-1} \frac{H[x(t)]}{x(t)} \quad \textbf{(5.6)}$$

Equation 5.4 is supported by the Bedrosian theorem (Xu and Yan, 2006):

$$H[a(t)\cos\phi(t)] = a(t)\,H[\cos\phi(t)]$$

The assumption involved here is the independence of frequency in *a*(t) and Cos [ϕ(t)], which correspond to narrow band hypothesis (Feldman, 2001). Furthermore, the narrow band hypothesis is equivalent to assume the inequality (Goswami and Hoefel, 2004):

$$|\phi'(t)| \geq \left|\frac{a'(t)}{a(t)}\right|$$

The instant frequency ν is an elementary tool for our purposes, and can be constructed as follows:

$$\nu(t) = \frac{1}{2\pi}\frac{d\,\phi(t)}{dt} \quad \textbf{(5.7)}$$

The computational achievement of 5.4 to 5.6 is uncomplicated (Sprott, 2003).

In summary, all the methods are designed to characterize the quasi-cyclic fluctuation of the MSD signal and lead to a supported dynamical interpretation (Fig. 5.1).

6. Dynamical variables from reanalysis

The composite analysis involves identifying and averaging one or more categories of fields of a variable selected according to their association with key conditions. The results of these composites are then used to generate hypotheses for patterns that may be associated with the individual scenarios.

Dynamical variables are needed to understand persistent flood and drought episodes since are usually accompanied by persistent atmospheric conditions and large-scale dynamical support (Mo *et al.*, 1997). During summer, threat of thunderstorm development over eastern of PTV region is a daily occurrence. Isolated or scattered airmass thunderstorms can be triggered by daytime surface heating. These events are usually short lived. The convective system occurs in associations with mesoscale or synoptic-scale disturbances, which may interact with diurnal heating. These disturbances include tropical cyclones, midlatitude fronts and see-breeze fronts. Attempts to study these events have been limited by the lack of consistent datasets.

The intense rainfall may lead to some flooding in urban areas, plains and crops fields contiguous to winding rivers. In contrast, an interruption of rainy conditions may reduce the quality on some crops, like maize (Contreras, 2003). The dryness tends to reduce soil moisture and increase surface heating, with some reduction in the local evaporation.

The reanalysis provides valuable data for studies of multiple flood and drought events since it is produced with a fixed assimilation system and a large input database. The model and procedures used in the NCEP–NCAR reanalysis are documented in Kalnay et al. (1996). Evaluation of large scale aspects of the hydrological cycle revealed by reanalysis (Mo and Higgins 1996) indicates that the analysis products are generally quite realistic, especially in the data-rich Northern Hemisphere.

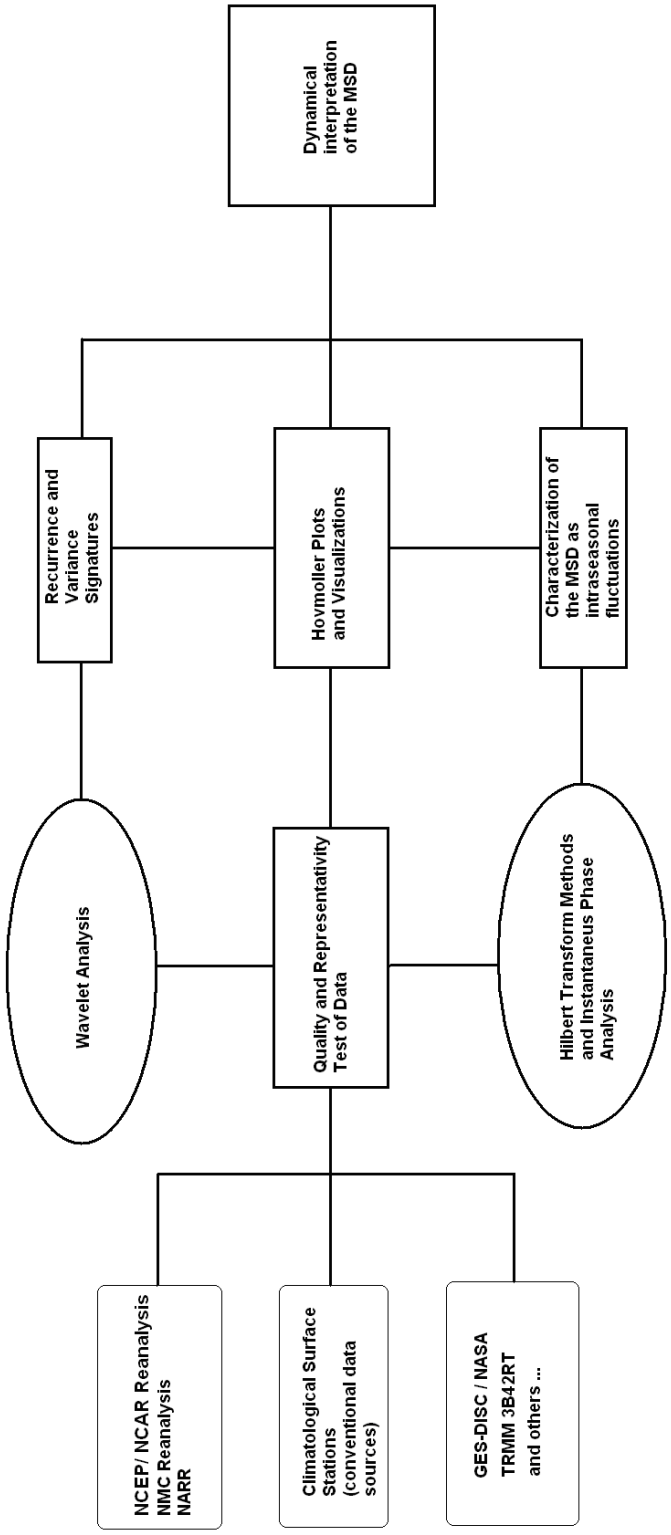

Fig. 5.1 Methodology proposed

7. Discussion

We first examine variations of rainfall in a coarse scale and for all four seasons. To provide a basis for further discussion on the characteristics of temporal fluctuations of precipitation, we illustrate in Fig. 7.1 the monthly mean precipitation amounts over the PTV region from NCEP/ NCAR data. There a large seasonal fluctuations and a wide range of variability. In addition, is clear that exist a strong annual cycle in the variance of precipitation. The precipitation has a strong seasonal dependence as compared with other regions in North America. From this view, convective-scale activity is almost masked. More precisely, intense and short events are embedding within synoptic activity. The shape and mean slope in plot suggest that wintertime precipitation fluctuations are mainly associated with synoptic scales and the summertime fluctuations are more related to shorter timescales.

The largest records in rainfall are related to the high incidence of tropical disturbances and hurricanes, both in Pacific coast and Gulf-Caribbean sector are the most important features of convective rainfall. In the decadal perspective, midsummer convective activity fluctuates around 85 mm per month (Fig. 7.2). From 1979 to 2006 a spatially coherent interdecadal evolution of summer rainfall is reveled. Statistically significant separation of two low frequency bands that represent independent information about spatially correlated oscillatory signals –the interdecadal and the decadal/quasidecadal signals- is obtained. Hurricane activity and other tropical systems from Atlantic and Pacific exert influence on interanual fluctuations, showing strong decadal variability. Also interdecadal and decadal signals join the ENSO and quasi-biennial signals in determining dominant patterns of natural climate variability.

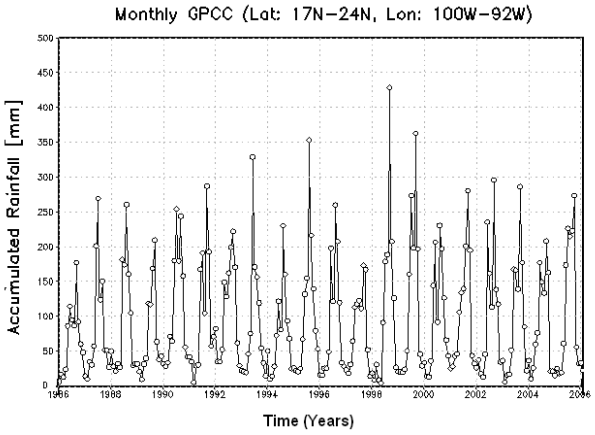

Fig. 7.1 Accumulated rainfall between from 1986 to 2006. Averages values are centered in the PTV region, showing large seasonal fluctuations.

The MSD drought was found as recurrence signature projected in several variables, accumulated rain, rain rate, wind speed, cloudiness, outgoing long wave radiation and lightning (Alvarez, 2002). In 1979-1980 rainfall data (Fig. 7.3) a reduction of a rain rate after July was originate, except near 96o W, where a maximum is located.

A more detailed latitudinal section reveals a modulation of accumulated rain up to 21o N (Fig.7.4) in the 1994 summer. The reduction of MSD is clearly different with respect to July anomalies (labeled 1 y 2). Rainfall pattern in fall (3) is less pronounced, and the transition summer-fall is frequently fuzzy. MSD is apparently connected with this seasonal variability. In contrast rainy episodes during the spring are sparse.

Other cases of rainfall plots confirm a wide range of temporal behavior of MSD (Figures 7.5 and 7.6).

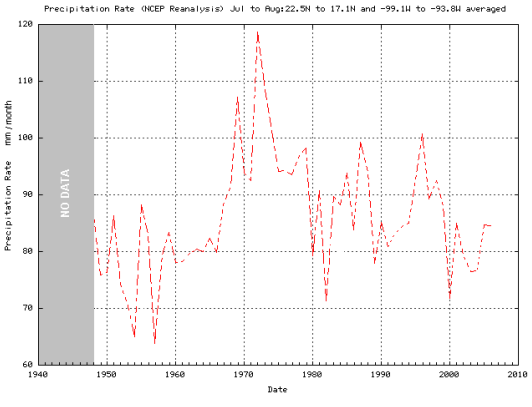

Fig. 7.2 Decadal variations in precipitation rate during summer.

Bimonthly composites indicate some connection with the local reduction of continentally, induced by the southwestern region of Gulf of Mexico and the Isthmus of Tehuantepec (Fig. 7.7). In this temporal scale the MSD signature is roughly noticeable, but is sufficient to show that the moisture source is allied with the ITCZ and the Caribbean coast of Belize. An interesting feature in the rainfall time series was found using a higher temporal resolution. A wet spells progression of three day duration seems appear during the MSD period (Fig. 7.8).

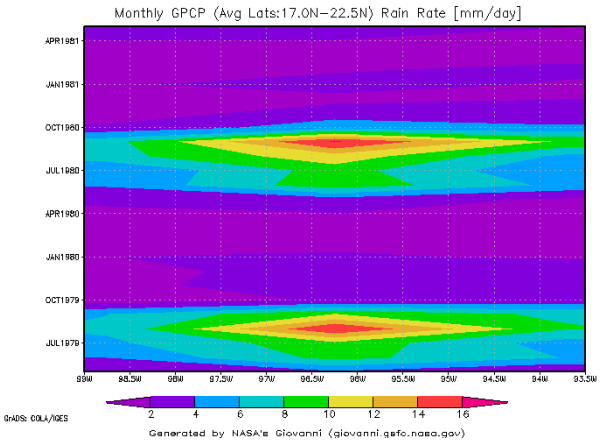

Figure 7.3 Hovmoller plot displaying longitudinally rain rate patterns in the biannual period 1979-80. MSD is present in the 1979 summer.

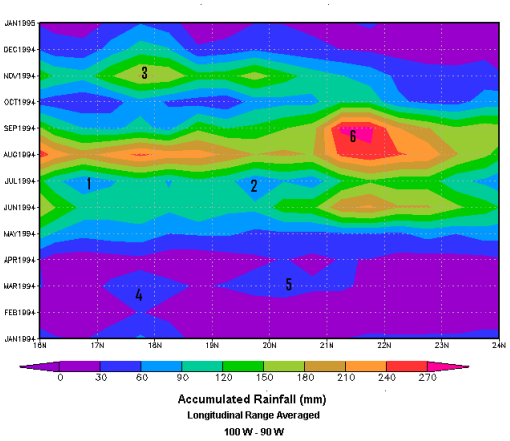

Fig. 7.4 Hovmoller plot displaying latitudinal accumulated rain patterns in the 1994 summer. See text for details.

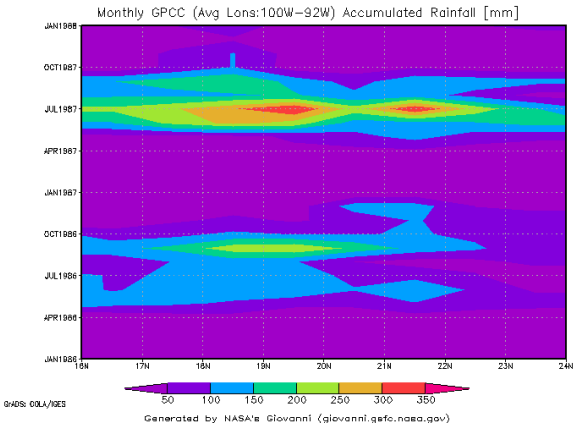

Fig. 7.5 Hovmoller plot displaying latitudinal accumulated rain patterns in the biannual period 1986-87.

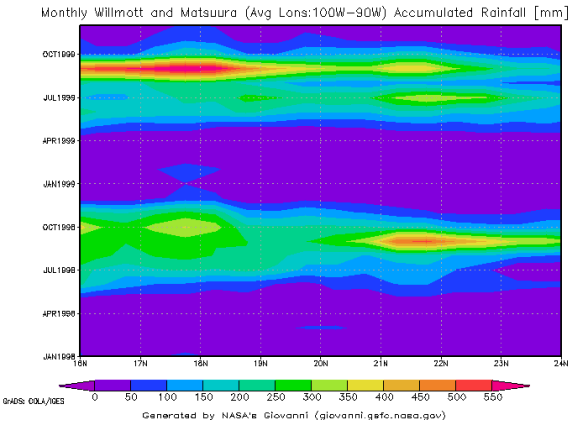

Fig. 7.6 Hovmoller plot displaying latitudinal accumulated rain patterns in the biannual period 1998-99.

These wet and dry events are fairly evenly distributed throughout the summer. Daily rainfall variability exerts very small influence in the annual amount of precipitation. Seasonality is preserved since coherence range result in a limited trend. This would lead one to expect than more careful and quantitative studies of the relationship of seasonality to other climate variables could be done using numerical models.

High resolution rainfall data at temporal scales varying from weekly to daily or even hourly is a very important problem in hydrological consequences of MSD. Wet spells progressions reveals strong seasonality, lack of gaussianity, space-time disaggregation and non-stationary. All these features are highly complex and poorly explored.

Despite the strong interanual variation in the number of wet and dry periods, some similarities exist. Common characteristics include: (i) wet spells usually occur after May 15th, (ii) wet spells are least frequent in July, and (iii) dry spells occur during the first two weeks in august. The increase in the percentage of stations reporting wet spells during MSD coincides with the northward migration of the ITCZ and occurrence of easterly waves in Caribbean Sea.

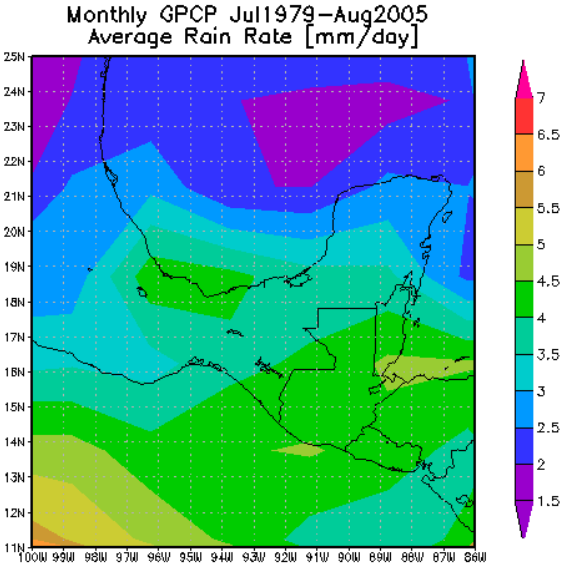

Fig. 7.7 Rain rate over the southeastern México (july-august average). The instability of air masses over eastern Pacific are linked with the southern Gulf of Mexico and Caribbean convective systems. Source: Ges-disc Interactive Online Visualization and Analysis Infrastructure GIOVANNI / NASA.

a)

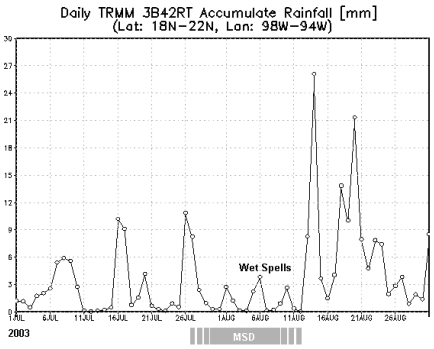

b)

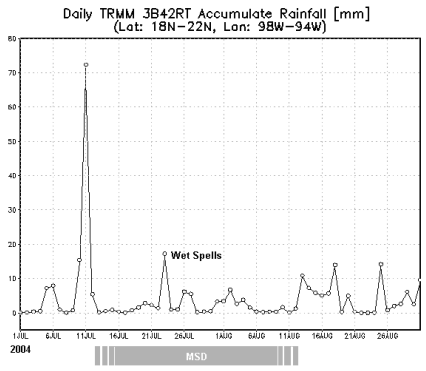

c)

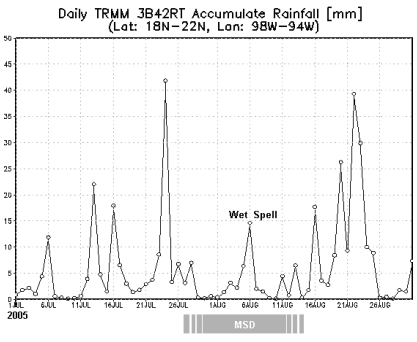

d)

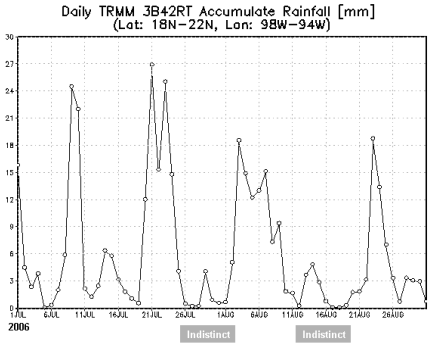

Fig. 7.8 Wet spells progression during some summers (years 2003 to 2006) observed in a spatial windows centered in 20° N, 96° W. Light rain interruptions (**a**) of about 4 mm is distributed in period of two pentads. Some episodes (**b** and **c**) exhibit fewer interruptions and eventually an indistinct MSD condition. Source: 3-hourly TRMM dataset from Ges-disc Interactive Online Visualization and Analysis Infrastructure GIOVANNI / NASA.

A Lat-Lon composite using 3-hourly accumulated rainfall data (Fig. 7.9) show a narrow corridor of low precipitation near a two convective systems. The thunderstorm over sea is placed just above the Papaloapan river outlet, and is formed during the early morning. Convective system at south (17.5° N, 95.5° W) is emerged from synoptic features like a tropical wave or disturbances derived from ITCZ or Caribbean Sea, near to the coast of Belize. Under an intense wind shear profile, the thin region **1** collapses.

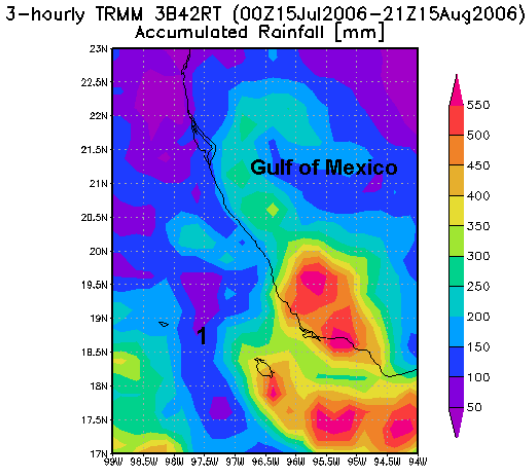

Fig. 7.9 Lat-Lon composite using a 3-hourly accumulated rainfall data. Transversal tiny region (**1**) with very low precipitation is shaped from 19.5°N, 97.5°W to 17.5° N. 97° W. Convective systems over ocean and land emerged from synoptic and sea-breezes features. Source: Ges-disc Interactive Online Visualization and Analysis Infrastructure GIOVANNI / NASA.

Longitudinal averaging (100° W to 90° W) composites of HODS reveals connectivity of temporal domains in latitude. The temporal behavior of very low precipitation domains (enclosed by grey dot line) show a regular intermittency (Fig. 7.10a) and bounded by a constriction at 22°N. The intense MSD episode is quite interesting (Fig. 7.10b), since a connection of zero rainfall is located at 16°N during august 9. Indistinct mode (Fig. 7.10c) exhibits an anticipated dryness pentad in july 26, and no constriction in latitude. The major rain-bearing system for the main rainy season (June to September) is the Inter Tropical Convergence Zone (ITCZ). On the other hand, the eastward moving midlatitude troughs will facilitate the interaction between the mid-latitude cold air and the tropical warm air so that unstable conditions will be created for the moisture that comes into eastern Mexico.

The global variance of the rainfall time series in the PTV region (see Fig. 7.11) show a minimum (marked as **2**) in the recurrence during august (month=8). The magnitude of variance (10^2) is equal to the dry season variance, but shorter in time (three pentads). The first maximum (**1)** is associated with the onset of wet season mostly derived from the tropical perturbations. The second maximum (**3**) is linked with the inter-annual periodicity, since correspond to the twelve month. A high variance (10^3) is typical to tropical rainfall scenarios.

During MSD episodes surface temperature rises due cloudiness anomaly. This effect introduce an opposite variance trend (Fig. 7.12). This statistical feature of extreme events in daily air temperature is an important aspect in the climate analysis, since these features affect various spheres of human activities including agricultural production, agricultural greenhouse design, human comfort, and domestic energy consumption. For the purpose of this study a warm spell is defined as the condition where daily maximum temperatures are running a given amount above normal for a minimum period of 48 h.

From the point of view of large-scale dynamics, the PTV region may be considered as homogeneous as a first approximation. Over this region the spatial variation of the air temperature during different seasons arises mainly from the effects of orographic barriers. With the intention of proving the stability of these numerical computations, an expansion of the dataset space window was designed. This experiment consists in obtaining the global wavelet for three nested regions A, B and C. Region A is centered in the PTV region. Region B y C are larger, as pointed in table 7.1

Region	Longitude	Latitude
A	260.6 to 268.1° E	23.8 to 16.2° N
B	258.8 to 270.0 ° E	25.7 to 14.3 ° N
C	256.9 to 271.9 ° E	27.6 to 12.4° N

Table 7.1 coordinates of spatial window expansion experiment.

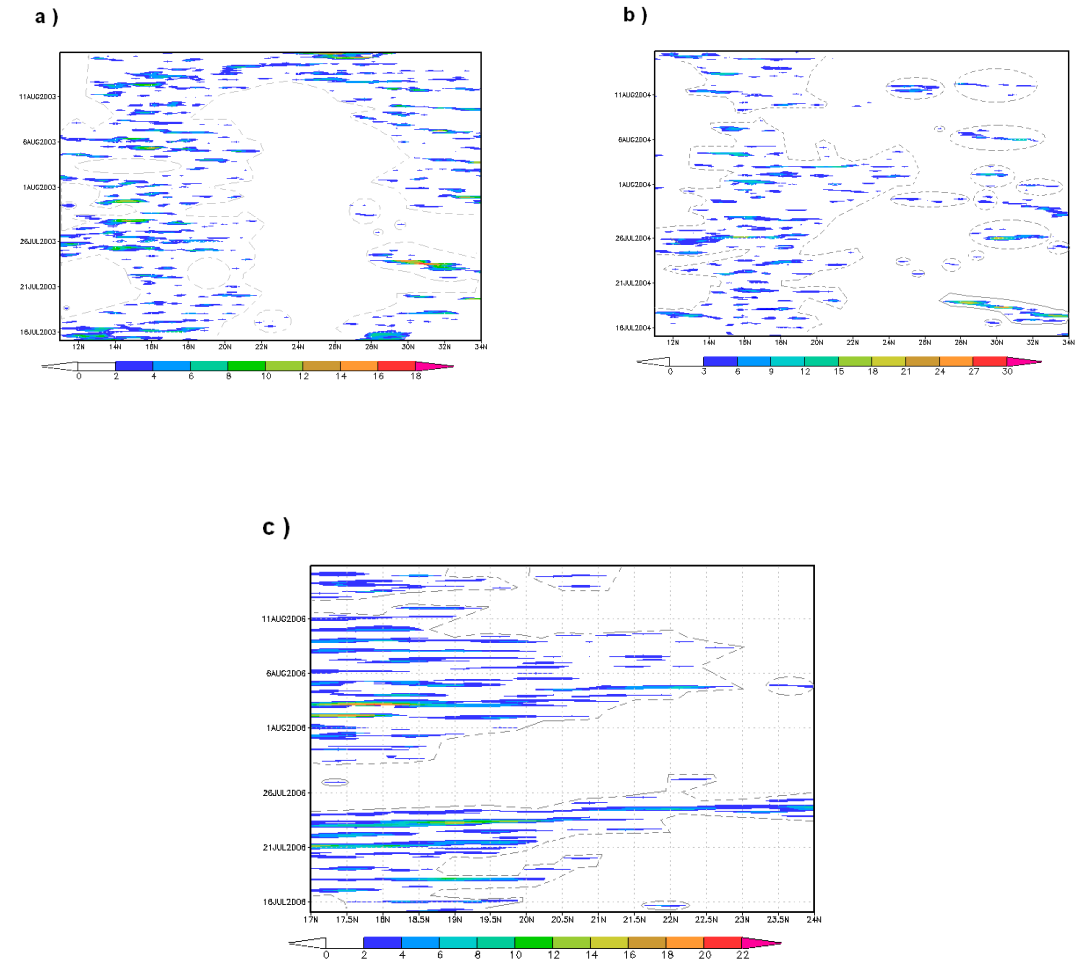

Fig. 7.10 Longitudinal averaging computation of Hovmoller diagrams reveals connectivity of temporal domains respect to latitude. In (**a**) wet spells are regular and constricted at 22°N. (**b**) Intense MSD episode. (**c**) Indistinct mode of MSD. Source: Ges-disc Interactive Online Visualization and Analysis Infrastructure GIOVANNI / NASA.

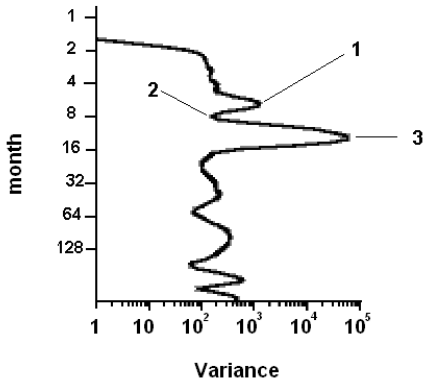

Fig. 7.11 Time-variance plot derived from WAN of the rainfall time series (33-years). Source: NARR dataset

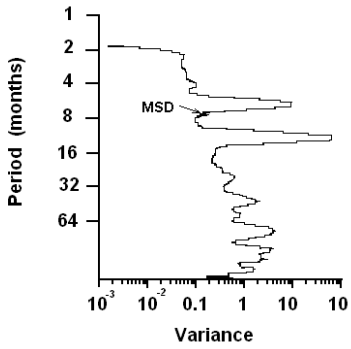

Fig. 7.12 Time-variance plot derived from WAN of the surface temperature time series (33-years). Source: NARR dataset

Small changes in the intraseasonal variance can be found (Fig.7.13). The aspects of shorter variability ([1], [2], [3] and [4]) practically preserved their periods, whereas the terms of variability between 2 and 5 years ([5] to [10]) experienced more variations in their variance.

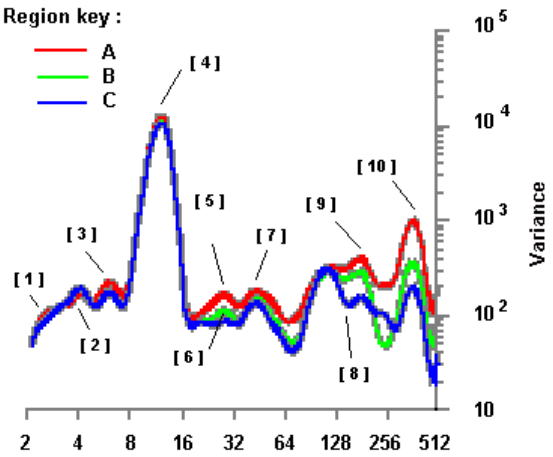

Fig 7.13 See text for details.

Daily summertime rainfall in Tlaxcala city shows a coherent behavior of the phase (Fig. 7.14). Humid and dry periods reveal mutual consistency. Restricting the analysis to dry events, one can found [1] no-linearity at beginnings of the summer, [2] changes of sign in midsummer and [3] cuasilinearity and phase low values at the end of the summer. In beginnings of the autumn rainfall has associate a time-dependant oscillating phase. These characteristics offer an alternative, trouble-free and efficient interpretation of MSD temporal structure. Using a broader time-scale (Fig. 7.15) mean monthly modulation frequency expressed in equation 5.7 reveals some interanual MSD signatures. Tendencies during spring results connected harmonically with the afterward MSD modulation shape. Crop damage in PTV region was reported in these years, being 1965 the year with greater losses by the drought. Calculations with the numerical algorithm of the FIH (Vandenhouten and Grebe, 1996) show specifically, that during august appears a non-linear intraseasonal oscillation.

Another important result was obtained from HT analysis, since an unexpected phase shift (UPS) prior to the summer are strongly associated with MSD missing episodes (Fig. 7.16). Analysis of binarized Hilbert phase time series suggests that knowledge of the behavior of precipitation on one timescale can be used to diagnose an indistinct MSD in broad scale. However, the coarse horizontal resolution of the data is a limitation in concluding whether this result is a true phenomenon.

The prediction of MSD is useful for agricultural and water resource use planning. However, the monitoring of crop yield requires a shorter event scale since it is often not the amount of seasonal rainfall that is important, but rather the steadiness of rainfall supplied by repeated wet or dry spells (Peña and Douglas, 2002) that is crucial to high crop yields. A dynamical view of the MSD suggests that an increase in drought conditions was observed in most of the southeastern and western parts of the country (Mendoza et al., 2006). During August, showery weather with some heavy rainfall events were concentrated across northern and central Mexico, while abnormally dry to moderate drought conditions in Baja California spread southward into Baja California Sur. Abnormally dry conditions also increased along the Pacific coast from Nayarit southward into Guerrero. This dryness along the southwest coast of Mexico was due, in part, to decreased tropical storm activity near the coast and a southward suppressed ITCZ. Along the Gulf of Mexico watershed, an abnormally dry region developed near Campeche Bay during July, and this dryness spread all along the Gulf coast, from central Tamaulipas through Veracruz and into Tabasco.

Another dry region developed from southern Chiapas into most of the Yucatan Peninsula. This pronounced dry trend indicated that the mid-summer drought, was more intense than average. Changes in August include a general improvement of the long-term dryness in North and Northwest México. The extreme and exceptional drought area in southern Sonora and northern Sinaloa eroded; although most of these regions frequently remain under abnormally dry to moderate drought conditions. No major improvements were observed in Nayarit or northwestern Sonora where a small area of extreme drought remains south of the international border. In northeastern Mexico, long-term dryness continues. A moderate drought area was introduced from southern Tamaulipas to central Veracruz, where agricultural impacts were reported over the Huasteca region. In addition, abnormally dry to moderate drought was also introduced over the Tehuantepec Isthmus.

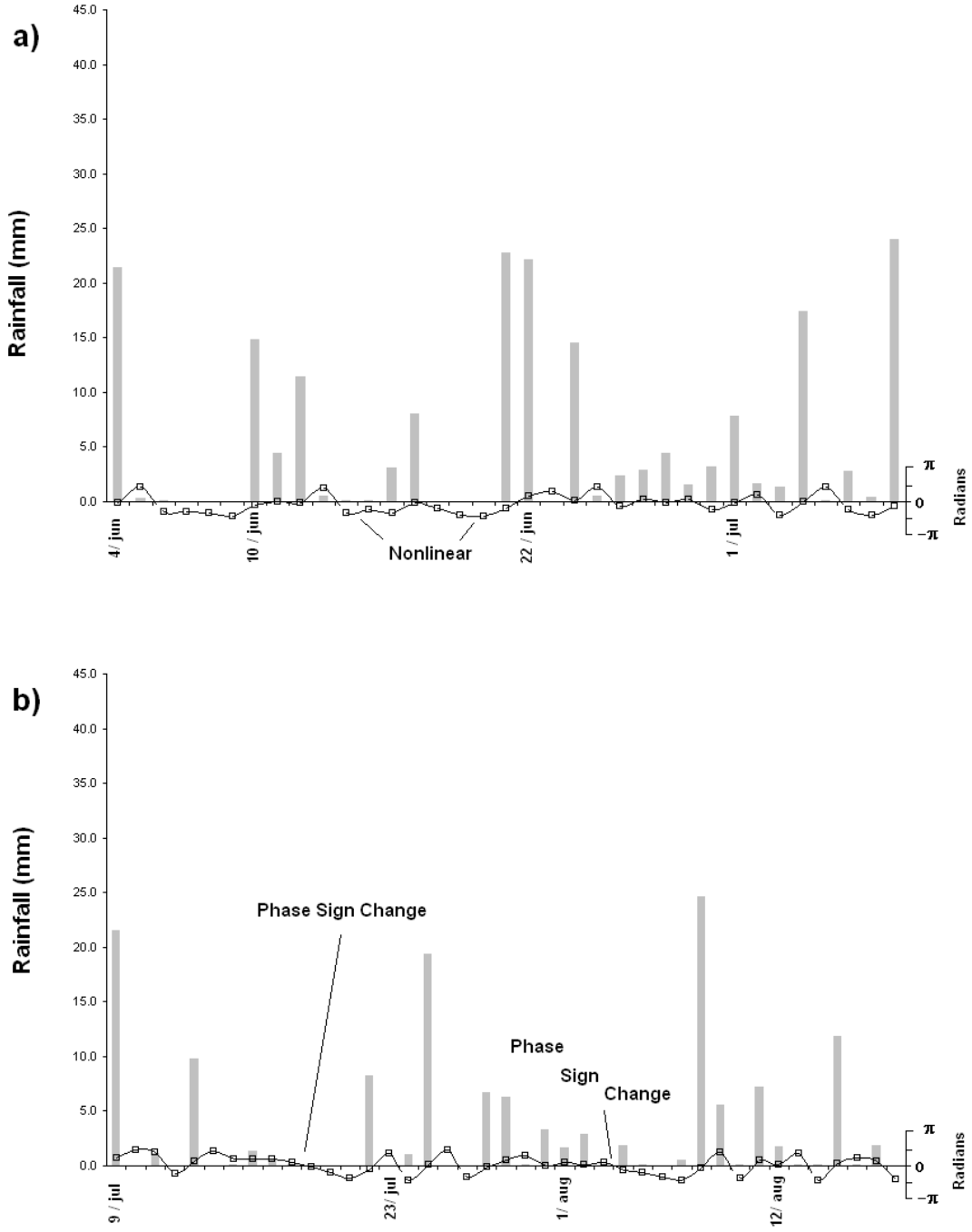

Fig. 7.14 (a) Daily rainfall (bars) and its computed phase (smoothed line) for Tlaxcala city (96° 14'W,19°19'N) during 1990. The instantaneous phase at the onset of wet season was highly coherent with progressive dry and wet spells. Nonlinear tendency from the phase in the daily scale is the most representative attribute. During middle summer (b) phase sign changes are the most prominent signatures.

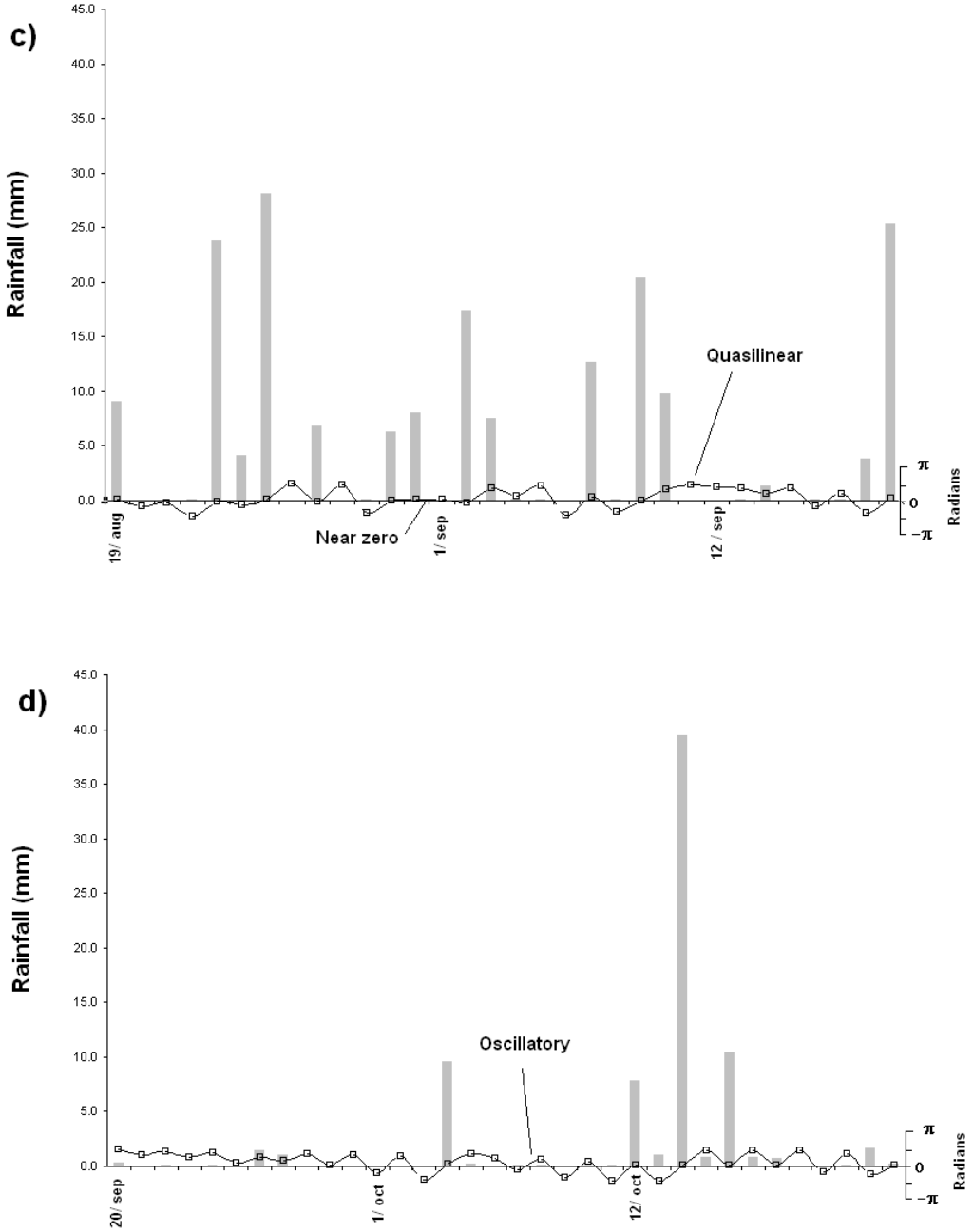

Fig. 7.14 (c) Daily rainfall (bars) and its computed phase (smoothed line) for Tlaxcala city (96° 14'W,19°19'N) during 1990. In summer's second half, near zero values of the phase (scale at right) were obtained and as well a quasi-linear tendency. At fall onset (d) oscillatory behavior result in a noticeably feature. Data source: ECET.

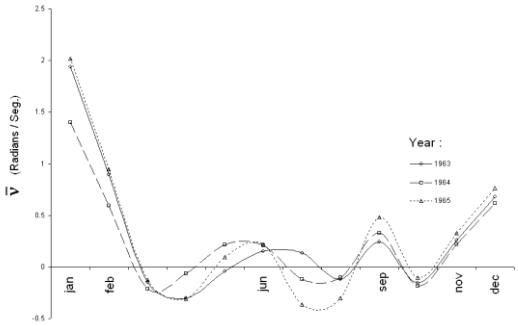

Fig. 7.15 Mean monthly modulation frequency computed with few historical records for Tehuacan (Lat: 18.48°, Lon: 97.40°). Tendencies during spring (April) are connected harmonically with the afterward MSD modulation shape.

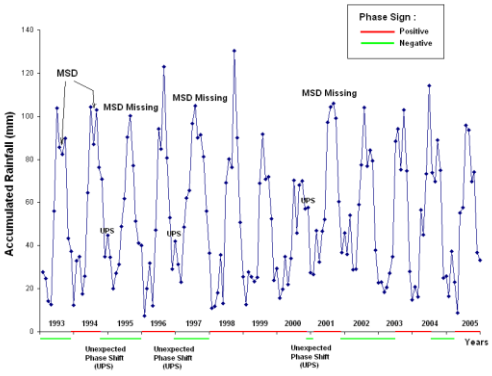

Fig. 7.16 Accumulated rainfall from NARR dataset in PTV region and phase sign intervals associated with MSD occurrence. HT analysis plus binarized phase time-series reveals that UPS acts as a precursor signal in broad spatial scale.

The meridional wind was generally southerly over PTV region at the 700-hPa level during the dry spells, whereas it was northerly during the wet spells. Characteristics of the ITCZ over the region are complicated by the topographic inhomogeneity and the associated thermally induced mesoscale circulations that make the ITCZ patterns near the earth's surface very subtle.

In order to expand upon the temporally and spatially limited observations collected, we examine continental-scale, multiple wet-season east–west regime changes in wind vertical structure over the latitudinal belt across central Mexico. It is interesting to note that the submonthly timescale changes in 850 HPa-wind between the regimes represented in Fig. 7.17 are coherent with agricultural yields. The impact of MSD over crop yields result highly correlated with kinematics features of zonal wind at 850 HPa. Severe effects in the yield (Tons/Hectare) of the maize were reported in the summer of 2004 within PTV region. This denominated condition as "very intense" also it was observed during midsummer of 2000. The speed pattern show wind oscillations around value -5 m/s. The global climate in 2000 was again influenced by the long-running Pacific cold episode (La Niña) that began in mid-1998. The La Niña was also associated with a well-defined African easterly jet located north of its climatological mean position and low vertical wind shear in the tropical Atlantic and Caribbean. Precipitation patterns influenced by typical La Niña conditions were associated with little rainfall in the central tropical Pacific and drier-than-normal conditions along the Gulf coast of the United States.

The denominated case "intense" reveals a pattern around -3.5 m/s with greater dispersion, as in 1994 and 2003 years. In the "moderate" case of MSD, zonal wind fluctuations are about 0.3 m/s, as in 1998-99 and 2005. In the case where MSD is absent (1995, 2001 years), sample fluctuations around 10 m/s with very short dispersion.

From special interest is the indistinct case (1996, 2006). In this case, the observed coherence of MSD is very low. This appears in 1996 and 2002 years. The values of the zonal component are alternated between -3.5 m/s and 6 m/s. Mature cold-episode conditions persisted across the tropical Pacific from November 1995 through May 1996 and contributed to large-scale anomalies of atmospheric circulation, temperature, and precipitation across the Tropics, the North Pacific and North America. Strong tropical intraseasonal (Madden-Julian oscillations) activity was observed during most of the year. The impact of these oscillations on extratropical circulation variability was most evident late in the year in association with the downstream circulation, temperature, and precipitation patterns over the eastern North Pacific and central North America. Other regional aspects of the short-term climate during 1996 included severe drought across the southwestern United States.

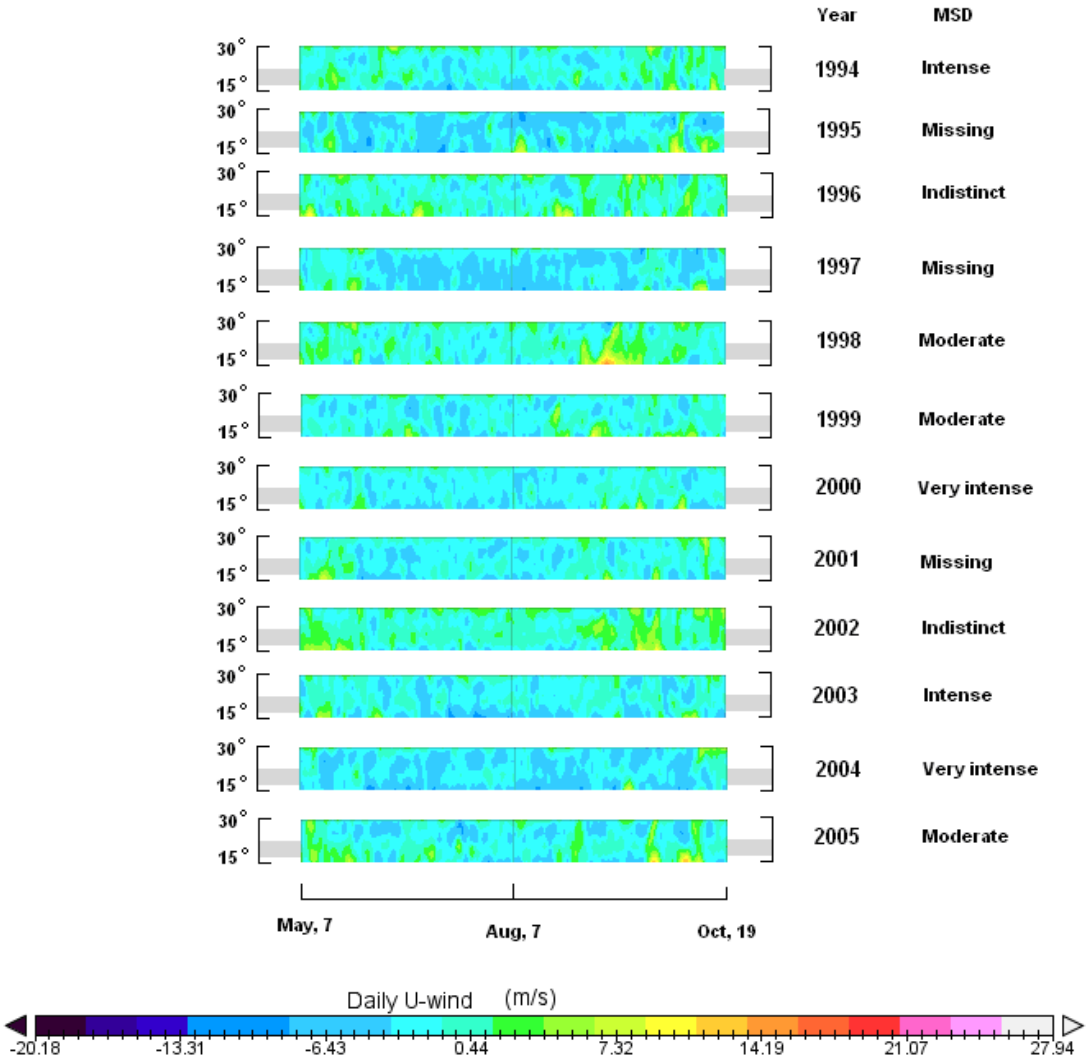

Fig. 7.17 Daily zonal wind (m/s) at level 850 HPa. Grey bands indicate latitudinal belt across central Mexico that contains region of interest. Right column express the MSD severity index based in damage crops reports. Source: NARR datasets and agricultural councils of state governments. Source: NARR datasets

This confirms the presence of synoptic-scale controls on regional-scale variability in convective vertical structure. Convective vertical structure and convective rainfall rates are all more pronounced during easterly regimes over the southern Mexico. Importantly, when considered with case study results from WAN and HT analysis, the systematic differences in convective structure that occur as a function of regime suggest that associated regime differences may exist in the vertical distribution of diabatic heating. Hence the discrimination of convective vertical structure ‘‘regimes’’ over parts of the PTV region and vicinity based on a resolved variable such as the 850 HPa zonal wind speed, while far from being perfect, may have important applications to the problems of rainfall estimation, and retrievals of latent heating.

The key processes in this theoretical framework seem to be evaporation–wind feedback, the SST-feedback, and the feedback between the monsoon-driven east–west circulation and ocean thermocline variations. It is shown that the interactions of these processes can provide a plausible physical mechanism to develop the spatial and temporal structure of the observed MSD in eastern Mexico. On a seasonal timescale, changes in Mexican convective structure are likely modulated by changes in the thermodynamic and dynamical structure of the troposphere associated with transitions between wet and dry seasons.

8. Conclusion

A different approach to MSD in eastern Mexico has been presented. It includes a rational and critically arguments. The present study has revealed the following:

- Statistical methods HT and WAN allowed to discover the fine structure of the MSD in the summer rain, with respect to the temporary variability.

- The traditional hydrometeorological approach of the MSD, based on the monthly average rain deficit during July-August was surpassed by the interpretation based on the no-linearity of the Hilbert phase.

- The instantaneous phase of rain allows simplifying the analysis of the interanual variability, making correspond to the synoptic fluctuations with the summer’s seasonality.

- The behavior of the phase in the scale of the order of a day reached a high degree of consistency in the analyzed cases. This consistency postulates expectations oriented to the operation of the numerical algorithm of the HT, like instrument of diagnosis and prediction.

- In the hi-res approach, the global wavelet of the temperature of the air displays fluctuations induced by the cloudless skies and the transitory answer of the water steam and the humidity of the ground.

- The levels of coherence between dry events, short as much long, allow to regionalization the agricultural impact of the MSD. This regionalization is congruent with the irregular distribution of the intraseasonal fluctuations.

- Data with finer horizontal resolution might reveal more dominance of convective scales in summer. More effort is needed to develop interactions of energy in several scales.

- The strength of statistical relationships linking atmospheric circulation to local and regional rainfall amounts are likely to depend on the time scale involved. The results confirm the feasibility of the approach but a monthly time scale is relevant in a climatological rather than hydrological context.

Acknowledgments. This research was made possible only through the support of the authorities of the Universidad Veracruzana and the facilities of the Center of the Atmospheric Sciences at the National University of Mexico and Apizaco Institute of Technology, during a sabbatical year. The NCEP/ NCAR reanalysis data was provided trough internet download. Thanks to M. Sc. Ana Delia Contreras for encourages, useful comments and some wavelet routines writes in Scilab.

9. References

Alvarez, O. 2002: Caracterización de la actividad eléctrica sobre los golfos de México con el sistema LIS/ TRMM. Tesis de Maestría en Ciencias Geofísicas. TESIUNAM 000301916, Universidad Nacional Autónoma de México.

Anctil, F. y P. Coulibaly 2004: Wavelet Analysis of the Interannual Variability in Southern Québec Streamflow. Journal of Climate: Vol. 17, No. 1 pp. 163–173

Bojariu, R. and Giorgi, F. 2005 The North Atlantic Oscillation signal in a regional climate simulation for the Europan region. Tellus A, Vol. 57, 4, 641-653.

Contreras, A. D. 2003: Aplicación de la ondeleta de Paul en los hidrometeoros de impacto en el cultivo del maíz bajo las fases del ENSO, en el Estado de Veracruz. Tesis de Maestría en Ciencias Geofísicas. TESIUNAM 000320921. Universidad Nacional Autónoma de México.

Coulibaly, P. y D.H. Burn 2005: Spatial and Temporal Variability of Canadian Seasonal Streamflows. Journal of Climate: Vol. 18, No. 1 pp. 191–210

Duffy, D. G. 2004: The Application of Hilbert–Huang Transforms to Meteorological Datasets. Journal of Atmospheric and Oceanic Technology 21, 599-611.

Feldman, M. 2001: Hilbert Transforms. Encyclopedia of Vibration, Academic Press, pp. 642-648.

Ghil, M., Allen, M. R., Dettinger, M. D., Ide, K., Kondrashov, D., Mann, M. E., Robertson, A. W., Saunders, A., Tian, Y., Veradi, F. y Yiu, P. 2002: Advanced spectral methods for climatic time series. Rev. Geophys., 40, 1, 1-41.

Giannini, A., Kushnir, Y. y Cane, M. A. 2000: Interannual Variability of Caribbean Rainfall, ENSO, and the Atlantic Ocean. Journal of Climate 13, 297-311.

Goswami. J.C. y Hoefel, A. E. 2004: Algorithms for estimating instantaneous frequency. Signal Processing 84, 1423-1427.

Greenland, D. 2005: Climate Variability and Sugarcane Yield in Louisiana. Journal of Applied Meteorology 44, 1655-1666.

Hegerl, G. C., Francis, Z., Peter, S. y Viatcheslav, K. 2004: Detectability of Anthropogenic Changes in Annual Temperature and Precipitation Extremes. Journal of Climate 17, 3683-3700.

Joseph, R., Ting, M. and Kumar, P. 2000 Multiple-scale spatio-temporal variability of precipitation over the coterminous United States. Journal of Hydrometeorology, Vol. 1, 5, 373-392.

Jury, M.R. and Pathak, B. 1991 A study of climate and weather variability over the tropical southwest Indian Ocean. Meteorology and Atmospheric Physics, Vol. 47, 1, 37-48.

Kalnay, E., and Coauthors, 1996: The NCEP/NCAR 40-year reanalysis project. Bull. Amer. Meteor. Soc., 77, 437–471.

Kayano MT and Kousky VE. 1999. Intraseasonal (30–60 day) variability in the tropics: principal modes and their evolution. Tellus 51A: 373–386.

Larson J, Zhou Y, Higgins RW 2005: Characteristics of Landfalling Tropical Cyclones in the United States and Mexico: Climatology and Interannual Variability. Journal of Climate: Vol. 18, No. 8 pp. 1247–1262.

Lau, K. M. y Weng, H. 1995: Climate signal detection using wavelet transform: how to make a time series sing. Bull. Amer. Meteor. Soc. 76, 12, 2391-2402.

Madden, R.A., and P.R. Julian, 1994: Observations of the 40–50-Day Tropical Oscillation—A Review. *Mon. Wea.* Rev., 122, 814–837.

Magaña V., J.A. Amador and S. Medina 1999: The Midsummer Drought over Mexico and Central America. Journal of Climate: Vol. 12, No. 6 pp. 1577–1588.

Martius, O., Schwierz, C. and Davies, H.C. 2006 A refined Hovmoller diagram. Tellus A 58 (2), 221-226

Matthews AJ. 2000. Propagation mechanisms for the Madden–Julian oscillation. Quarterly Journal of the Royal Meteorological Society 126: 2637–2651.

Mélice, J. L., Coron, A. y Berger, A. 2001: Amplitude and Frequency Modulations of the Earth's Obliquity for the Last Million Years. Journal of Climate 14, 1043-1054.

Mendoza, B., Velasco, V. y Jáuregui, E. 2006: A Study of Historical Droughts in Southeastern Mexico. Journal of Climate, 19, 2916-2934.

Mesinger, F., DiMego, G., Kalnay, E., Mitchell, K., Shafran, P. C., Ebisuzaki, W., Jovic, D., Woollen, J., Rogers, E., Berbery, E. H., Ek, M. B., Fan, Y., Grumbine, R., Higgins, W., Li, H., Lin, Y., Manikin, G., Parrish, D., Shi, W. 2006: North American Regional Reanalysis. Bulletin of the American Meteorological Society 87, 343-360.

Mo, K. C., and R. W. Higgins, 1996: Large-scale atmospheric water vapor transport as evaluated from the NCEP/NCAR and the NASA/DAO reanalyses. J. Climate, 9, 1531–1545.

Mo KC, Paegle JN, Higgins RW (1997) Atmospheric Processes Associated with Summer Floods and Droughts in the Central United States. Journal of Climate: Vol. 10, No. 12 pp. 3028–3046

Mwale, D. y Gan, T. Y., 2005: Wavelet analysis of variability, teleconnectivity and predictability of the September-November East Africa rainfall. Journal of Applied Meteorology, 44,2, 256-269.

Nielsen-Gammon JW 2001: A Visualization of the Global Dynamic Tropopause. Bulletin of the American Meteorological Society: Vol. 82, No. 6 pp. 1151–1167

Nolin, A.W and Hall-McKim, E. A. 2006. Frequency modes of monsoon precipitation in Arizona and New Mexico. Monthly Weather Review, 134, 12, 3774-3781.

Pavia EG, Graef F, Reyes J 2006: PDO–ENSO Effects in the Climate of Mexico. Journal of Climate: Vol. 19, No. 24 pp. 6433–6438

Peña, M. y Douglas, M. W. 2002 : Characteristics of Wet and Dry Spells over the Pacific Side of Central America during the Rainy Season. Monthly Weather Review 130, 3054-3073.

Picinbono, B. 1997: On instantaneous amplitude and phase of signals, IEEE Trans. Signal Process., 45, 1, 552-560.

Salinas, J. A. 2006: Dinámica de Ondas del Este y su interacción con el flujo medio en el Caribe. Tesis Doctoral. Universidad Nacional Autónoma de México, 93 págs.

Santos, C. A., Galvao, C. O., Susuki, K. y Trigo, R. M. 2001 Matsuyama city rainfall data análisis using wavelet transform. Annual Journal of Hydraulic Engineering, JSCE, Vol. 45.

Sprott, J.C. 2003: Chaos and Time-Series Analysis. Oxford University Press. New York.

Torrence, C. and Compo, G.P. 1998 A practical guide to wavelet analysis. Bull. Amer. Meteor. Soc., 79, No. 1,61-78

Vandenhouten, R. and R. Grebe 1996: SANTIS (Systems ANalysis and TIme Series Processing) - ein Werkzeug zur Analyse von Biosignalen. Biomedizinische Technik. Biomedical Engineering. 41: 364.

Waylen, P.R., C.N. Caviedes, and M.E. Quesada, 1996: Interannual Variability of Monthly Precipitation in Costa Rica. *J.* Climate, 9, 2606–2613.

Xu, Y. y Yan, D. 2006: The Bedrosian identity for the Hilbert Transform of product functions. *Proc. Amer. Math.* Soc. 134, 2719-2728.